

Article

Tribological Study on Photocatalysis-Assisted Chemical Mechanical Polishing of SiC

Hyunseop Lee 

Department of Mechanical Engineering, Dong-A University, Busan 49315, Republic of Korea; hyunseop@dau.ac.kr; Tel.: +82-51-200-7648

Abstract: Silicon carbide (SiC) is widely used as a power semiconductor substrate material, even if it takes a large amount of processing time to secure an appropriate surface as a wafer for devices after chemical mechanical polishing (CMP). Therefore, studies on SiC CMP have focused on shortening the processing time by increasing material removal efficiency. Among the methods of SiC CMP that have been widely studied recently, the photocatalysis-assisted CMP (PCMP) method is known to efficiently increase the material removal rate (MRR) of SiC under UV light and photocatalysts. However, a limited number of comparative studies have been conducted on PCMP from a tribology perspective. In this article, a comparative study was conducted from a tribology perspective on CMP, mixed abrasive slurry CMP (MAS CMP), and PCMP. The experimental results demonstrated that SiC PCMP has higher friction and processing temperature than MAS CMP and general CMP, which may be caused by photocatalytic oxidation and the TiO₂ particles used as photocatalysts.

Keywords: silicon carbide (SiC); chemical mechanical polishing (CMP); photocatalyst; tribology

1. Introduction

Various materials with different physical and electrical properties are emerging as semiconductor substrates in addition to silicon (Si), which has traditionally been used as a substrate for semiconductors. With diverse semiconductor devices emerging, the interest in silicon carbide (SiC), which is used in opto-electric, high-power or high-frequency, and high-temperature devices, has been increasing [1–3]. In wafer manufacturing, chemical mechanical polishing (CMP) removes the subsurface damage caused by wafer shaping and surface processing after ingot growth and ensures surface roughness of several nm or less [4]. However, due to its high hardness and chemical stability, SiC requires a significant amount of processing time in CMP, which utilizes both chemical reactions and mechanical material removal [4,5]. The long CMP process time increases the price of SiC and imposes environmental burdens. Researchers have been conducting various studies to increase the material removal efficiency of SiC CMP.

There are two main approaches to increasing mechanical material removal efficiency in SiC CMP: (1) improving the material removal efficiency through abrasive particles and (2) enhancing chemical reactivity. The use of a mixed-abrasive slurry containing abrasives of different types has been introduced as a method to improve the mechanical material removal efficiency in SiC CMP. Lee et al. [6] performed a study using a mixed abrasive slurry (MAS) containing 120 nm colloidal silica particles and 25 nm nano-diamonds for CMP of 6H-SiC substrates. They presented the CMP material removal rate (MRR) as the weight change per unit time and achieved an MRR of 0.5 mg/h and surface roughness (Ra) of 0.24 nm. However, scratches were still observed after CMP, owing to the use of diamond particles. Lee and Jeong [7] conducted a MAS CMP experiment on SiC using 120 nm colloidal silica and 30 nm diamond particles. They created indentation marks on the SiC substrate using nanoindentation and observed the changes in the marks after CMP. They showed that MAS CMP removed the indentation marks more effectively than CMP



Citation: Lee, H. Tribological Study on Photocatalysis-Assisted Chemical Mechanical Polishing of SiC.

Lubricants **2023**, *11*, 229. <https://doi.org/10.3390/lubricants11050229>

Received: 26 April 2023

Revised: 13 May 2023

Accepted: 16 May 2023

Published: 18 May 2023



Copyright: © 2023 by the author. Licensee MDPI, Basel, Switzerland. This article is an open access article distributed under the terms and conditions of the Creative Commons Attribution (CC BY) license (<https://creativecommons.org/licenses/by/4.0/>).

using only colloidal silica slurry and stated that the hard abrasives (diamond) in the MAS are responsible for the mechanical removal of SiC, whereas the soft abrasives (colloidal silica) have the effect of reducing surface roughness. Lee et al. [8] performed atomic force microscopy (AFM) scratching tests using silicon tips and silicon tips coated with diamond and confirmed that SiC when chemically reacted with slurry, had a higher wear volume than non-reacted SiC. Additionally, it was experimentally confirmed that MAS CMP shows higher frictional force than SiC CMP using only colloidal silica slurry.

Currently, the most widely studied method for increasing the chemical reactivity in SiC CMP is photocatalysis-assisted CMP (PCMP). PCMP is known to activate chemical reactions during CMP via photocatalytic oxidation. Photocatalytic oxidation by TiO₂ photocatalysts is primarily utilized in PCMP. When light energy (ultraviolet; UV) above the band gap of TiO₂ is irradiated, electrons and holes are generated on the surface of TiO₂, leading to the formation of superoxide ion through the reaction between electrons and oxygen (O₂) on the photocatalyst surface, and hydroxyl radicals (\cdot OH) are generated through the reaction between holes and water (or moisture). The chemical reaction between SiC and \cdot OH through photocatalytic reaction can be expressed as follows [9]:



The early reported SiC polishing technique using UV light employed UV light alone without using photocatalysts [10]. Kubota et al. [11] improved the efficiency of SiC CMP by adding hydrogen peroxide (H₂O₂), which is capable of electron trapping, to the slurry and utilizing UV light. Ohnishi et al. [12] proposed SiC PCMP using anatase TiO₂ photocatalyst and controlled the gas environment in the CMP machine. They showed that the MRR increased when utilizing UV light in an oxygen atmosphere. Zhou et al. [13] proposed PCMP using polishing pads coated with TiO₂ particles and experimentally demonstrated that the MRR of SiC increased with increasing TiO₂ concentration. Yuan et al. [14] used H₂O₂ and potassium ferrate (K₂FeO₄) as electron trapping agents and experimentally demonstrated that H₂O₂ has higher electron trapping performance than K₂FeO₄. In their study, the slurry with pH 2 and the inclusion of TiO₂ and H₂O₂ showed the highest MRR. Lu et al. [15] showed that coating TiO₂ particles on nanodiamonds could improve surface roughness and enhance the low MRR in SiC CMP. Yan et al. [16] demonstrated that the results of PCMP can vary depending on the H₂O₂ and TiO₂ concentration and the pH, and UV intensity in the slurry. In their study, the optimal conditions for achieving the highest MRR were observed at a UV intensity of 1000 mW/cm², H₂O₂ concentration of 4.5 vol.%, TiO₂ concentration of 3 g/L, and pH of 11. However, in Wang's PCMP study [17] using a slurry of nano-alumina particles and TiO₂ with potassium persulfate (K₂S₂O₈), the highest MRR was observed at a K₂S₂O₈ concentration of 3 wt.%, TiO₂ concentration of 0.2 wt.%, and slurry pH of 6.

Many studies have been conducted on SiC PCMP, and most of them have focused on the effects of TiO₂ photocatalyst on MRR and surface roughness reduction. However, no studies have been conducted on the effect of mechanical material removal caused by the addition of TiO₂ particles to the existing slurry and on the tribological behavior of PCMP in the presence of UV light. In this study, the tribological characteristics in PCMP of 6H-SiC were investigated. To understand the material removal mechanism in TiO₂-based PCMP, MAS CMP using colloidal silica slurry with TiO₂ particles was performed without UV irradiation along with PCMP experiments under UV irradiation.

2. Materials and Methods

2.1. Sample Preparation

Before the CMP experiment, the surface of a 6H-SiC wafer with a 4-inch diameter was processed for 10 min via diamond mechanical polishing (DMP). The pressure during DMP was 400 g/cm², the rotation speed was 80 rpm, and the slurry flow rate was 4 mL/min. The diameter of diamond particles in the slurry (polycrystalline diamond, oil base) used in the experiment was 3 μm. Figure 1 shows the DMP machine used in the experiment, with

a platen diameter of 300 mm. After DMP, the SiC wafer was cleaned using an ultrasonic cleaner after removing the oil-based slurry with isopropanol alcohol. The wafer thickness was measured using a 3D surface metrology system (MicroProf 200, FRT GmbH, Bergisch Gladbach, Germany). The thickness of the SiC wafer before DMP was approximately $356.08 \pm 2.59 \mu\text{m}$.



Figure 1. DMP machine used for SiC wafer preparation.

The average MRR in SiC DMP was approximately $1.755 \pm 0.061 \mu\text{m}/\text{min}$. The surface roughness after DMP was measured using a 3D optical surface profiler (NewView™ 7300, Zygo Corp., Middlefield, CT, USA) at five points on the wafer. The surface roughness after SiC DMP was $R_z 92.903 \mu\text{m}$ and $R_a 6.132 \mu\text{m}$. Figure 2a,b show the MRR and surface roughness of SiC DMP for CMP experiments, respectively.

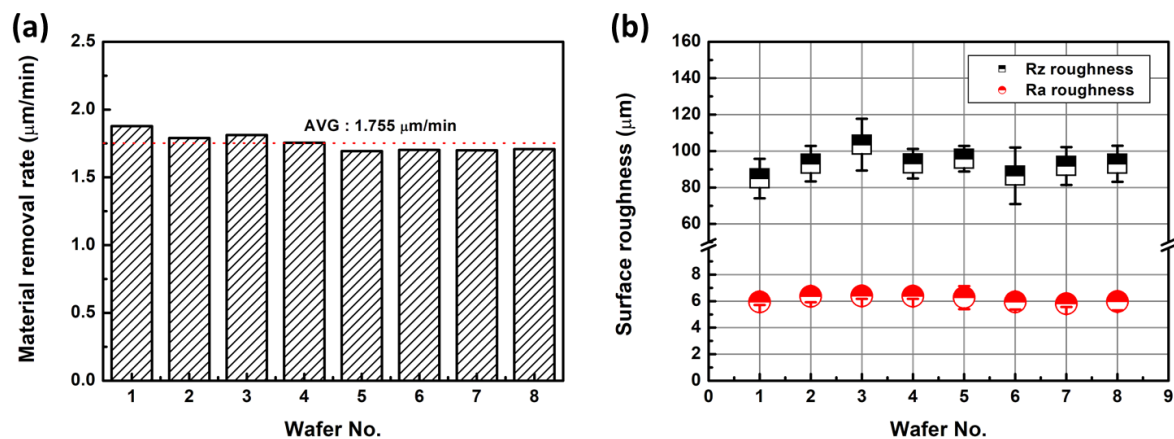


Figure 2. SiC DMP results: (a) material removal rate and (b) surface roughness.

2.2. PCMP Experiment

For the PCMP experiment, a UV irradiation system (200 W, 220 V, 1 Phase, 60 Hz, Air cooling, UVA) was installed in the CMP machine (POLI-400, G&P Technology, Busan, Republic of Korea) (Figure 3). Due to the MRRs during CMP, MAS CMP, and PCMP were expected to be extremely small, the MRR of SiC was calculated through the following equation by measuring the weight change of the SiC wafer before and after CMP using a precision scale (AS.220.R2, RADWAG, Radom, Poland).

$$MRR = \Delta m / \rho_{SiC} \cdot A \cdot t \quad (2)$$

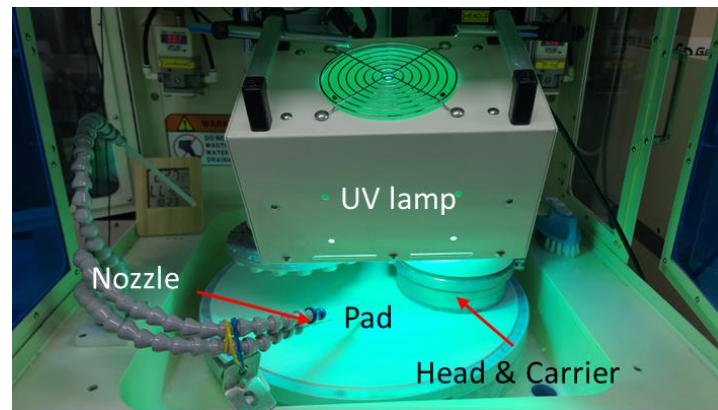


Figure 3. Photocatalysis-assisted CMP system.

Δm is the change in the mass of SiC wafer before and after CMP, ρ_{SiC} (3.21 g/cm^3) is the density of SiC, A is the surface area of SiC wafer, and t is the CMP time.

Table 1 lists the conditions of the PCMP experiment. In the experiment, a polyurethane-impregnated non-woven pad was used for CMP. The pressure during CMP, MAS CMP, and PCMP was 400 g/cm^2 , the rotation speed of the table and the head was 80 rpm, the slurry flow rate was 200 mL/min , and the slurry was circulated. A colloidal silica slurry was prepared for the experiment, and TiO_2 particles (AEROXIDE TiO_2 P25, Evonik, Essen, Germany) and H_2O_2 were used as the photocatalyst and electron trapping agent, respectively. TiO_2 photocatalysts are known to obtain energy above 3.2 eV, which is bandgap energy, in the UVA region. The diameters of the colloidal silica and TiO_2 particles are 72 nm and 25.4 nm, respectively. In the experiment, the particle content in the slurry was maintained at 32 wt%.

Table 1. Experimental conditions for PCMP.

Parameter	Condition
Pressure (g/cm^2)	400
Head and Table speed (rpm)	80
Slurry flow rate (ml/min)	200
Polishing time (min)	60, 120

In this study, the results of CMP using a colloidal silica slurry, MAS CMP using colloidal silica and TiO_2 particles together, and PCMP were compared. Table 2 lists the experimental cases in this study.

Table 2. Experimental cases.

Case	Condition
CMP	Colloidal silica (32 wt%)
MAS CMP	Colloidal silica (31.8 wt%) + TiO_2 (0.2 wt%) + H_2O_2 (6.0 wt%)
PCMP	Colloidal silica (31.8 wt%) + TiO_2 (0.2 wt%) + H_2O_2 (6.0 wt%) + UV light

The friction force in the CMP was measured by mounting a piezoelectric pressure sensor (Kistler Type 9135B, Kistler, Winterthur, Switzerland) at the back of the polishing head, and the pad temperature was measured using an infrared laser sensor (FT-H30, Keyence, Osaka, Japan) at the tracking edge of the polishing head. Signals from sensors were transmitted to the computer through an A/D converter and displayed on the computer screen in real time. The measuring frequency was 10 Hz. Before the start of the experiments, the temperature of the pad was maintained at about $19.5 \text{ }^\circ\text{C}$, and the break-in was conducted

using a dummy wafer for 1 h after attaching the new pad to the platen. The conditioning of the pad between the experiments was performed for 1 min using a brush.

In PCMP, the surface chemical reaction layer was measured using an X-ray photoelectron spectrometer (XPS, K-Alpha, Thermo Fisher Scientific, Waltham, MA, USA), and the SiC specimen was immersed in slurry while irradiating UV light for five days.

2.3. Electrochemical Experiment

A potentiostat (WPG100e, WonATech, Seoul, Republic of Korea) was used to analyze the electrochemical properties of the three types of slurry (Table 2) used in the experiment. A saturated calomel electrode (SCE) was used as a reference electrode, graphite was used as a counter electrode, and a 2-inch SiC wafer was used as a working electrode. UV light was installed outside the potentiostat and was irradiated to the slurry through a glass beaker. Figure 4 shows a schematic diagram of an electrochemical characteristic experiment using a potentiostat.

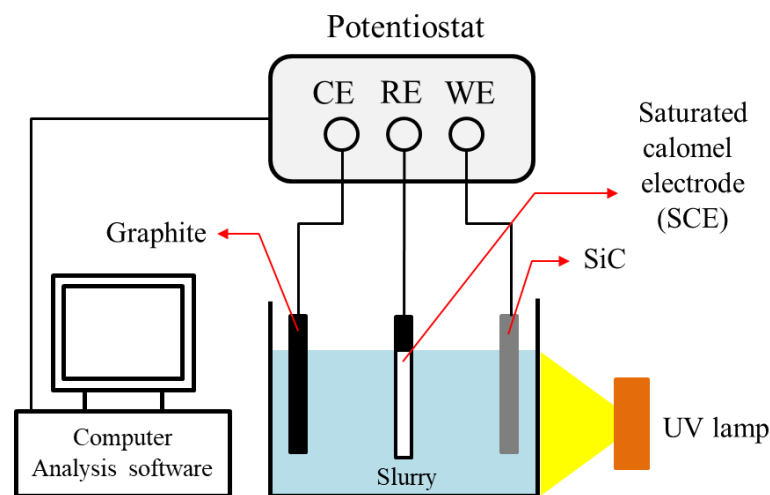


Figure 4. Electrochemical experiment using potentiostat.

3. Results and Discussion

3.1. Material Removal Rate

Figure 5 shows the MRRs for each experimental case. For 1 h long CMP, the MRR was 59.5 nm/h, which is extremely low owing to the high hardness and chemical stability of SiC. Although the abrasive concentration of the slurry used in this experiment was higher at 32 wt% than in typical CMP, it did not exhibit sufficient material removal efficiency. After CMP for 2 h, the MRR was 39.7 nm/h, which was lower than the CMP for 1 h. The decrease in MRR with an increase in the processing time may be due to the removal of the rough SiC surface after DMP by CMP, thereby lowering the surface roughness and removing the subsurface damaged layer.

The MAS CMP exhibited MRRs of 91.3 nm/h and 63.5 nm/h after 1 h and 2 h of processing, respectively, and showed higher MRRs than general CMP. During MAS CMP, the weight concentration of the total particles was the same as that of general CMP; however, 31.8 wt% of colloidal silica particles and 0.2 wt% of TiO₂ particles were included in the slurry. Because the TiO₂ particles used in the experiment are smaller than the colloidal silica particles, the total number of particles in the slurry was greater than that of the case where only 23 wt% of colloidal silica was used. In MAS CMP, the increase in MRR may be due to the increase in the total number of particles after adding the TiO₂ particles and the addition of H₂O₂ in the slurry.

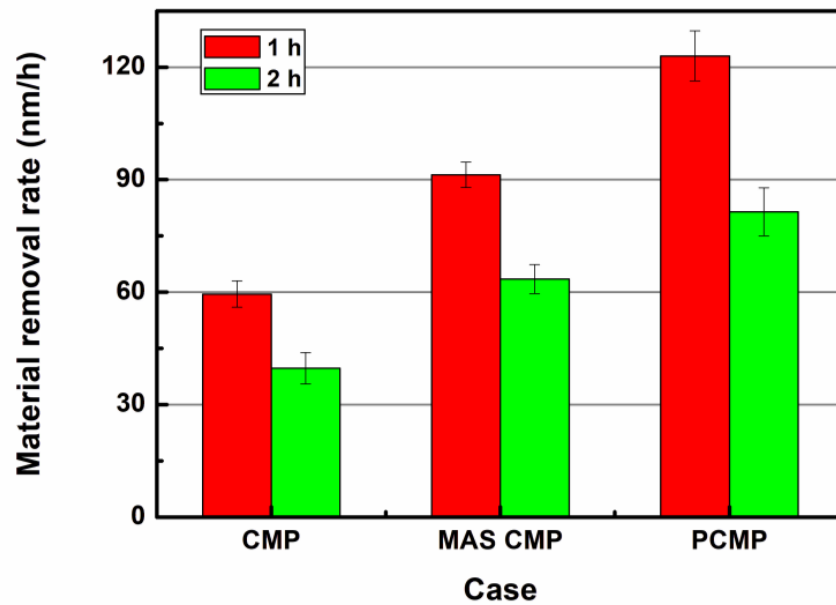


Figure 5. Material removal rate (MRR) of SiC during different CMP methods for 1 h and 2 h.

In PCMP, the UV light was irradiated to the slurry used in MAS CMP, and the MRR was higher than that of general CMP and MAS CMP. In PCMP, the MRRs for 1 h and 2 h were 123.0 nm/h and 81.4 nm/h, respectively. According to the experimental results shown in Figure 5, the high MRR in PCMP may be due to the improvement of mechanical material removal and chemical reaction by the addition of TiO₂ particles and photocatalytic oxidation by UV light irradiation.

From the results of the 1 h processing shown in Figure 5, the increase in MRR through MAS CMP with TiO₂ particles was 31.8 nm/h (approximately 53.5% increase over general CMP), and the MRR of MAS CMP was increased by 31.7 nm/h through PCMP (approximately 34.7% increase over MAS CMP). In the case of 2 h processing, the MRR of MAS CMP increased by 23.8 nm/h (59.9%) compared to general CMP, and in the case of PCMP, the MRR increased by 17.9 nm/h (28.2%) compared to MAS CMP.

3.2. Surface Roughness

Figure 6 shows the surface roughness reduction rate after 1 h and 2 h of CMP processing. The average surface roughness of SiC wafers before CMP was Rz 92.903 μm and Ra 6.132 μm, as stated in the experimental conditions. After 1 h of CMP processing, the surface roughness values of the SiC wafer were Rz 75.756 μm and Ra 5.722 μm, and the surface roughness reduction rates were Rz 17.250 μm/h and Ra 0.248 μm/h. In the case of MAS CMP, the surface roughness values after 1 h processing were Rz 49.354 μm and Ra 4.354 μm, and the surface roughness reduction rates were Rz 37.092 μm/h and Ra 1.594 μm/h. After 1 h of PCMP, the surface roughness values were Rz 39.584 μm and Ra 3.848 μm, and the surface roughness reduction rates were Rz 56.18 μm/h and Ra 2.416 μm.

After 2 h of general CMP, the surface roughness decreased to Rz 63.562 μm and Ra 5.463 μm. After 2 h of MAS CMP, the SiC surface roughness values were Rz 39.316 μm and Ra 3.456 μm, and in the case of PCMP, they were Rz 26.738 μm and Ra 2.687 μm. In the 2 h experiment, the Rz roughness reduction rates of CMP, MAS CMP, and PCMP were 14.722 μm/h, 23.565 μm/h, and 34.513 μm/h, respectively. In addition, the Ra roughness reduction rates of CMP, MAS CMP, and PCMP were 0.253 μm/h, 1.246 μm/h, and 1.788 μm/h, respectively. Therefore, the surface roughness reduction rate tends to decrease as the processing time increases, which may be due to the fine roughness present on the SiC surface and the decrease of the surface damaged layer. Figure 7a shows a SiC surface after DMP, and Figure 7b–d show SiC surfaces after 2 h of processing using CMP,

MAS CMP, and PCMP methods, respectively. In the case of PCMP, it is shown that the roughness present on the SiC surface after DMP is more effectively removed by the high MRR via the photocatalytic oxidation reaction.

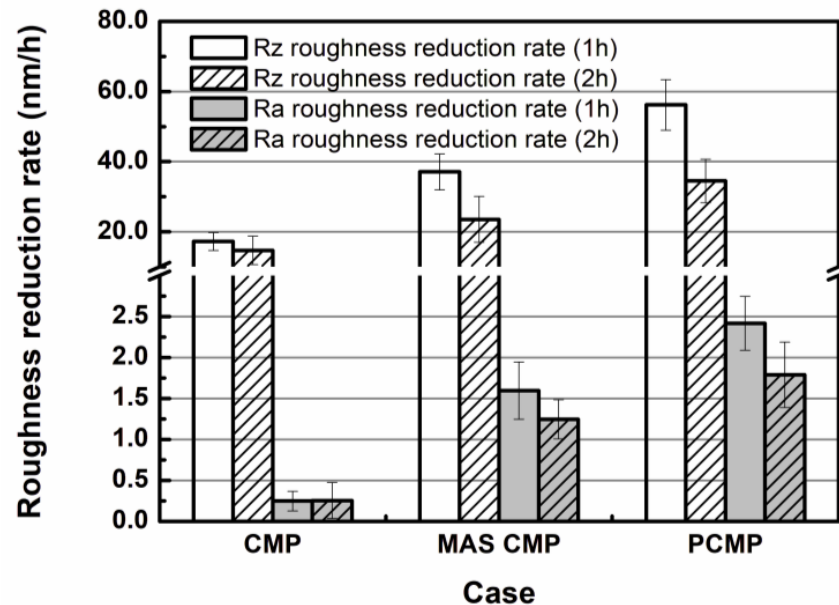


Figure 6. Surface roughness (Rz and Ra) reduction rate according to CMP methods.

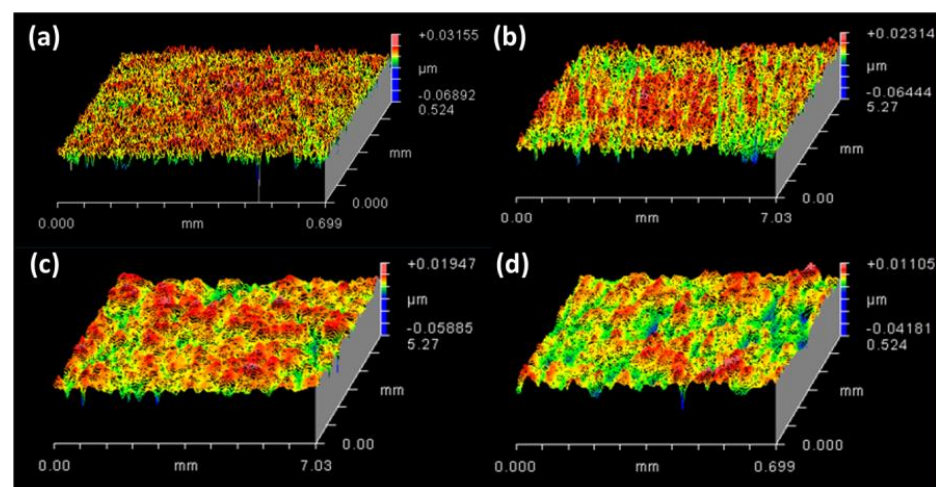


Figure 7. Surface roughness profiles of SiC wafers; (a) after DMP, (b) after CMP for 2 h, (c) after MAS CMP for 2 h, and (d) after PCMP for 2 h.

3.3. Electrochemical Analysis

In this study, Tafel analysis was conducted using a potentiostat to understand the electrochemical reaction characteristics between SiC and slurry. Figure 8 shows the Tafel plot in CMP, MAS CMP, and PCMP. When a general CMP slurry was used, the corrosion potential (E_{corr}) was -238.0 mV (SCE), and the corrosion current density (i_{corr}) was 0.54 $\mu\text{A}/\text{cm}^2$. In the case of the MAS CMP slurry, E_{corr} was 31.8 mV (SCE), and i_{corr} was 3.34 $\mu\text{A}/\text{cm}^2$. In the case of PCMP under UV light, E_{corr} and i_{corr} increased compared to MAS CMP and general CMP to 128.0 mV (SCE) and 6.88 $\mu\text{A}/\text{cm}^2$, respectively.

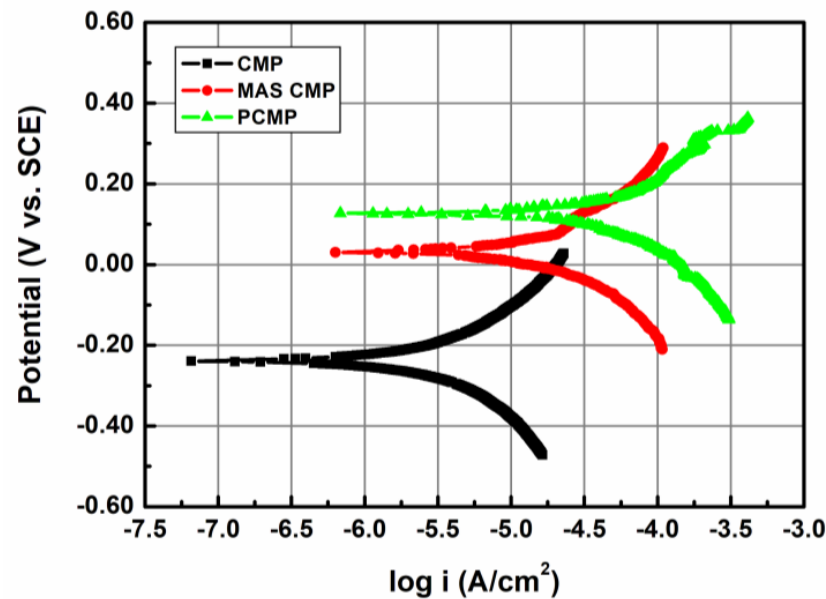


Figure 8. Tafel plots in CMP, MA CMP, and PCMP (Scan rate 10 mV/s, step potential 1 mV).

Because the CMP process has a material removal mechanism that removes the chemical reaction layer produced through the chemical reaction between the slurry and the material, MRR in CMP is related to the corrosion rate (CR). According to Faraday's law, CR has a linear relationship with i_{corr} . The following formula is the calculation formula of CR if the unit is mpy (mils/year) [18,19]:

$$CR = 0.13 \cdot i_{corr} \cdot EW / \rho, \quad (3)$$

where EW and ρ indicate equivalent weight and density, respectively.

In the Tafel analysis for CMP, MAS CMP, and PCMP conducted in this study, the CRs were 0.43545 mpy, 2.68801 mpy, and 5.53791 mpy, respectively. In the case of MAS CMP, in which TiO_2 particles and H_2O_2 are added to the colloidal CMP slurry, the CR increased potentially due to the oxidation of the SiC surface by H_2O_2 , which is an oxidizer. PCMP exhibited a significant increase in the CR due to the activation of chemical reactions by $\cdot\text{OH}$ radicals caused by photocatalytic oxidation by TiO_2 catalysts and UV light.

3.4. Friction Force and Temperature

CMP is a process in which interfacial friction by particles placed between wafers and polishing pads affects the MRR. Various factors affect the friction force in CMP, such as the material of the wafer, the characteristics of the polishing pad, the type of abrasive particles, and the pressure and speed during processing. In addition, the friction force of the CMP is also affected by the chemical reaction between the slurry and the wafer.

In this study, changes in frictional force and temperature in CMP, MAS CMP, and PCMP were observed, as shown in Figure 9. The friction force in a PCMP is higher than that in a general CMP and MAS CMP, and the MAS CMP showed a higher friction force than that in a general CMP. The friction forces at CMP, MAS CMP, and PCMP were 0.215 kN, 0.231 kN, and 0.248 kN, respectively. The friction forces shown in Figure 9 increase during the CMP and then gradually converge at the maximum friction force. The maximum frictional forces at CMP, MAS CMP, and PCMP were 0.243 kN, 0.260 kN, and 0.274 kN, respectively. The increase in friction in MAS CMP may be due to the oxidation of the SiC surface following the addition of H_2O_2 and the improvement of mechanical material removal by TiO_2 particles. The high friction force in PCMP seems to be the effect of the activation of chemical reactions by photocatalytic oxidation. In addition, in PCMP, it seems that high friction and MRR can more effectively planarize the rough SiC surface produced by DMP.

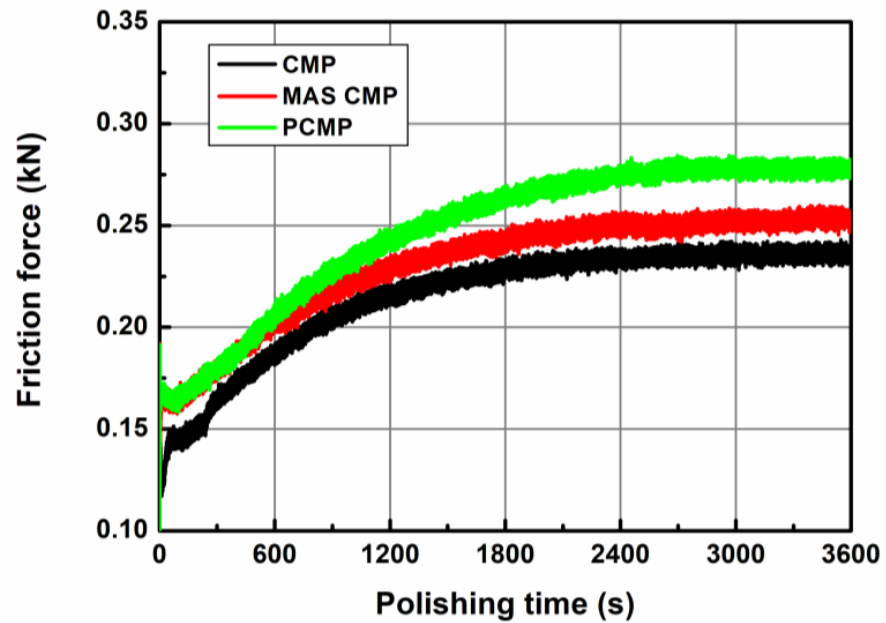


Figure 9. Changes in frictional force in CMP, MAS CMP, and PCMP.

Figure 10 shows the temperature changes during CMP, MAS CMP, and PCMP. The pad temperature before the start of the experiments was maintained at 19.5 °C. As shown in Figure 10, the temperature of the polishing pad was the highest in PCMP under UV light, and the general CMP showed the lowest temperature. The average temperatures of CMP, MAS CMP, and PCMP were 26.4 °C, 27.5 °C, and 29.7 °C, respectively. The temperature increases at CMP, MAS CMP, and PCMP were 9.40 °C, 10.41 °C, and 11.80 °C, respectively. The temperature in CMP is closely dependent on friction, and because this research conducted an experiment under the same pressure and rotation speed, it may be dependent on the material removal rate according to the CMP method. In addition, the high pad temperature during CMP is expected to help improve MRR by helping the chemical reaction between slurry and SiC wafers.

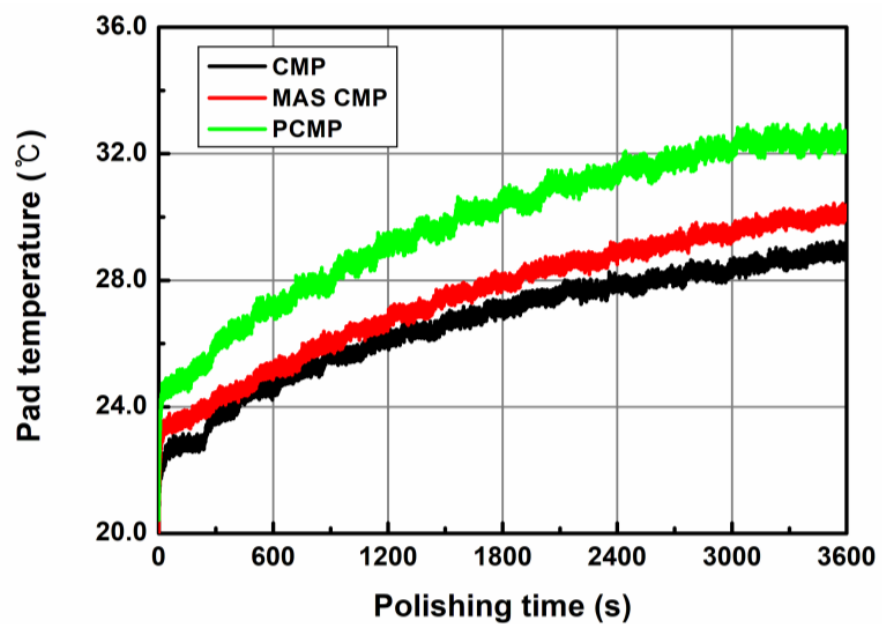


Figure 10. Changes in pad temperature in CMP, MAS CMP, and PCMP.

3.5. Material Removal Mechanism of SiC PCMP

In previous studies [14,20], the material removal mechanism of SiC PCMP is explained by the activation of chemical action by photocatalytic oxidation. Figure 11a shows the XPS measurement result of the as-received SiC wafer, and Figure 11b shows the XPS measurement result of the SiC wafer immersed in slurry for five days and irradiated under UV light. The increase in the O1s peak in Figure 11b from the XPS measurement results shows that the SiC surface can be oxidized during PCMP. The Tafel analysis results in Figure 8 also confirm that CR increases by photocatalytic oxidation during PCMP, and thus O1s peak can increase, as illustrated in Figure 11. In Figure 11, in the case of the PCMP condition, the C1s peak is shown to be decreased, and this seems to be a result of the photocatalytic oxidation of SiC and $\cdot\text{OH}$ in Equation (1).

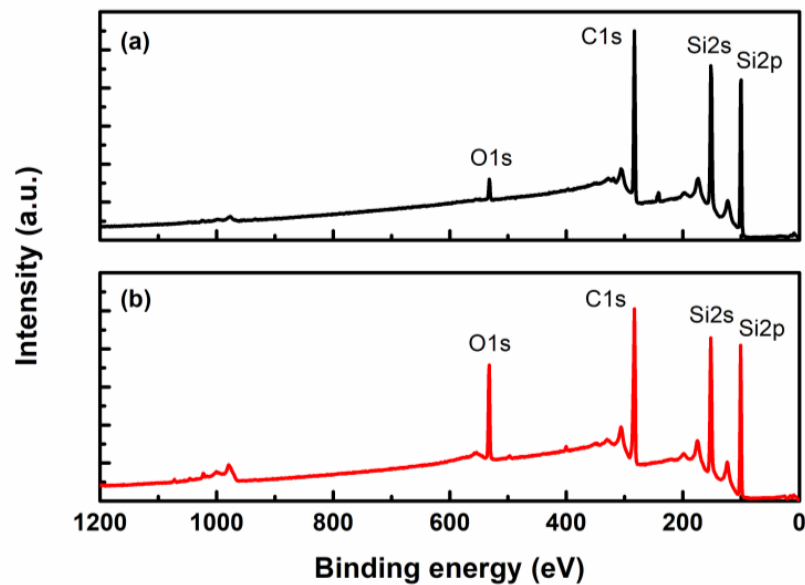


Figure 11. XPS results of SiC wafers; (a) as-received SiC wafer and (b) SiC wafer immersed in slurry for 5 days while irradiating UV light.

The surface of the oxidized SiC is removed by particles in the slurry, and the TiO_2 used as a photocatalyst also contributes to the material removal. In addition, the high frictional force and frictional heat generated during SiC PCMP may have resulted in a higher material removal efficiency than the general CMP that uses only colloidal silica particles. In addition, PCMP appears to rapidly reduce SiC surface roughness due to high friction, temperature, and MRR. Therefore, the high MRR of SiC PCMP may be the result of synergy with the tribology in CMP and photocatalytic oxidation, as shown in Figure 12.

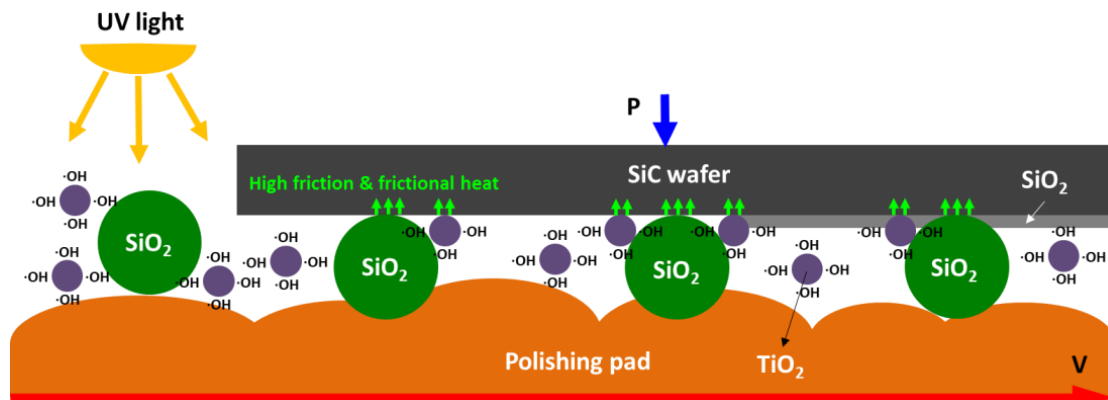


Figure 12. Material removal mechanism of SiC PCMP.

4. Conclusions

In this study, the techniques of SiC PCMP, MAS CMP containing colloidal silica particles (72 nm), TiO₂ particles (25.4 nm), and H₂O₂, and CMP using only colloidal silica were compared from a tribology perspective. When H₂O₂ and TiO₂ particles were added to the colloidal silica slurry, the MRR in SiC CMP increased, which may have been caused by the oxidation reaction of the slurry and SiC and the increase in the number of abrasive particles. In addition, higher friction force and temperature were measured in MAS CMP than in general CMP. Among the three CMP methods, the highest MRR, frictional force, and temperature were identified in PCMP under UV light and with TiO₂ particles (photocatalyst), which may have been due to photocatalytic oxidation. According to the Tafel analysis, the highest i_{corr} and CR were measured in PCMP, and the XPS analysis of the SiC surface confirmed that an oxide film that is relatively easier to remove mechanically than SiC was formed. Therefore, the material removal mechanism in PCMP could have involved mechanically removing the surface oxide layer formed by activating the photocatalytic oxidation reaction under UV light, photocatalysts, and the chemical reactions caused by the temperature rise.

Funding: This work was supported by the Dong-A University research fund.

Data Availability Statement: Not applicable.

Acknowledgments: This study was supported by the research fund of Dong-A University, and I would like to thank the Korea Institute of Industrial Technology (KITECH) for its help in experimenting and measuring.

Conflicts of Interest: The authors declare no conflict of interest.

References

1. Ma, G.; Li, S.; Liu, F.; Zhang, C.; Jia, Z.; Yin, X. A Review on Precision Polishing Technology of Single-Crystal SiC. *Crystals* **2022**, *12*, 101. [[CrossRef](#)]
2. Yasseen, A.A.; Zorman, C.A.; Mehregany, M. Roughness Reduction of 3C-SiC Surfaces Using SiC-Based Mechanical Polishing Slurries. *J. Electrochem. Soc.* **1999**, *146*, 327–330. [[CrossRef](#)]
3. Zhao, Q.; Sun, Z.; Guo, B. Material removal mechanism in ultrasonic vibration assisted polishing of micro cylindrical surface on SiC. *Int. J. Mach. Tools Manuf.* **2016**, *103*, 28–39. [[CrossRef](#)]
4. Grim, J.R.; Benamara, M.; Skowronski, M.; Everson, W.J.; Heydemann, V.D. Transmission electron microscopy analysis of mechanical polishing-related damage in silicon carbide wafers. *Semicond. Sci. Technol.* **2006**, *21*, 1709–1713. [[CrossRef](#)]
5. Zhou, L.; Audurier, V.; Pirouz, P. Chemomechanical Polishing of silicon Carbide. *J. Electrochem. Soc.* **1997**, *114*, L161. [[CrossRef](#)]
6. Lee, H.; Park, B.; Lee, H.; Jeong, S.; Seo, H.; Joo, S.; Jeong, H.; Kim, H. The Effect of Mixed Abrasive Slurry on CMP of 6H-SiC Substrate. *Mater. Sci. Forum* **2008**, *569*, 133–136. [[CrossRef](#)]
7. Lee, H.S.; Jeong, H.D. Chemical and mechanical balance in polishing of electronic materials for defect-free surfaces. *CIRP Ann.-Manuf. Technol.* **2009**, *58*, 485–490. [[CrossRef](#)]
8. Lee, H.S.; Kim, D.I.; An, J.H.; Lee, H.J.; Kim, K.H.; Jeong, H. Hybrid polishing mechanism of single crystal SiC using mixed abrasive slurry (MAS). *CIRP Ann.-Manuf. Technol.* **2010**, *59*, 333–336. [[CrossRef](#)]
9. Ishikawa, Y.; Matsumoto, Y.; Nishida, Y.; Taniguchi, S.; Watanabe, J. Surface treatment of silicon carbide using TiO₂(IV) photocatalyst. *J. Am. Chem. Soc.* **2003**, *125*, 6558–6562. [[CrossRef](#)] [[PubMed](#)]
10. Lee, H. Research Trends on Chemical Mechanical Polishing Using Ultraviolet Light. *Tribol. Lubr.* **2022**, *38*, 247–254.
11. Kubota, A.; Kurihara, K.; Touge, M. Fabrication of smooth surface on 4H-SiC substrate by ultraviolet assisted local polishing in hydrogen peroxide solution. *Key Eng. Mater.* **2012**, *523–524*, 24–28. [[CrossRef](#)]
12. Ohnishi, O.; Doi, T.; Kurokawa, S.; Yamazaki, T.; Uneda, M.; Yin, T.; Koshiyama, I.; Ichikawa, K.; Aida, H. Effects of Atmosphere and Ultraviolet Light Irradiation on Chemical Mechanical Polishing characteristics of SiC Wafers. *Jpn. J. Appl. Phys.* **2012**, *51*, 05EF05.
13. Zhou, Y.; Pan, G.; Zou, C.; Wang, L. Chemical Mechanical Polishing (CMP) of SiC Wafer Using Photo-Catalyst Incorporated Pad. *ECS J. Solid State Sci. Technol.* **2017**, *6*, P603–P608. [[CrossRef](#)]
14. Yuan, Z.; He, Y.; Sun, X.; Wen, Q. UV-TiO₂ photocatalysis assisted chemical mechanical polishing 4H-SiC wafer. *Mater. Manuf. Process.* **2017**, *33*, 1214–1222. [[CrossRef](#)]
15. Lu, J.; Huang, Y.; Fu, Y.; Yan, Q.; Zeng, S. Synergistic Effect of Photocatalysis and Fenton on Improving the Removal Rate of 4H-SiC during CMP. *ECS J. Solid State Sci. Technol.* **2021**, *10*, 044001. [[CrossRef](#)]
16. Yan, Q.; Wang, X.; Xiong, Q.; Lu, J.; Liao, B. The influences of technological parameters on the rate of ultraviolet photocatalytic reaction and photocatalysis-assisted polishing effect. *J. Cryst. Growth* **2020**, *531*, 125379. [[CrossRef](#)]

17. Wang, W.; Zhang, B.; Shi, Y.; Ma, T.; Zhou, J.; Wang, R.; Wang, H.; Zeng, N. Improvement in chemical mechanical polishing of 4H-SiC wafer by activating persulfate through the synergistic effect of UV and TiO₂. *J. Mater. Process. Technol.* **2021**, *295*, 117150. [[CrossRef](#)]
18. Seibi, A.C.; Rostron, P.; Elramady, A.; Mishra, B.; Nazer, O.A.; Ameri, A. Effect of Radial Expansion of Cr-Mo Steel Tubes on Their Corrosion Behavior in Sea Water. *Mater. Sci. Appl.* **2012**, *3*, 587–595. [[CrossRef](#)]
19. Sastri, V.S.; Ghali, E.; Elboudjaini, M. *Corrosion Prevention and Protection: Practical Solutions*; John Wiley & Sons, Ltd.: Hoboken, NJ, USA, 2007; p. 45.
20. Tanaka, T.; Takizawa, N.; Hata, A. Verification of the Effectiveness of UV-Polishing for 4H-SiC Wafer Using Photocatalyst and Cathion. *Int. J. Automot. Technol.* **2018**, *12*, 160–169. [[CrossRef](#)]

Disclaimer/Publisher's Note: The statements, opinions and data contained in all publications are solely those of the individual author(s) and contributor(s) and not of MDPI and/or the editor(s). MDPI and/or the editor(s) disclaim responsibility for any injury to people or property resulting from any ideas, methods, instructions or products referred to in the content.